6th ECCOMAS Conference on Smart Structures and Materials
SMART2013
Politecnico di Torino, 24-26 June 2013
E. Carrera, F. Miglioretti and M. Petrolo (Editors)
www.smart2013.com

MODELLING OF INTERGRANULAR AND TRANSGRANULAR CRACKING IN POLYCRYSTALLINE SILICON SOLAR CELLS

Marco Paggi, Mauro Corrado

Politecnico di Torino
Department of Structural, Geotechnical and Building Engineering
Corso Duca degli Abruzzi 24, 10129, Torino, Italy
e-mail: marco.paggi@polito.it, web page: http://staff.polito.it/marco.paggi
e-mail: mauro.corrado@polito.it, web page: http://staff.polito.it/mauro.corrado

Key words: Photovoltaics, Solar cells, Nonlinear fracture mechanics, Finite element method.

ABSTRACT

A computational method for the simulation of intergranular and transgranular cracking in Silicon solar cells is proposed. To model crack propagation, an interface element compatible with 2D plane stress linear triangular or quadrilateral continuum elements has been coded in the finite element programme FEAP. The constitutive relation of the element is formulated by using a cohesive zone model (CZM) accounting for Mixed Mode effects. To study how grain boundary and Silicon bulk properties influence the crack pattern, an intrinsic CZM strategy is pursued. Interface elements are automatically inserted in the FE mesh from the beginning of the simulation, preserving the geometry of the material microstructure (grain boundaries). Different fracture properties can be assigned to the interface elements placed along the grain boundaries or inside the grains. Numerical results show a prevalence of transgranular over intergranular cracking for a wide range of interface fracture properties, in general agreement with experimental observations. Grain boundary decohesion takes place only for very weak grain boundary toughness. Mesh refinement leads to smoother stress and displacement fields and a smearing out of strain localization. However, the crack pattern appears to be almost independent of mesh size.

INTRODUCTION

Photovoltaics (PVs) based on Silicon semiconductors is one the most growing technology in the World for renewable, sustainable, non-polluting, widely available clean energy sources. Commercial PV modules are composite laminates with very different layer thicknesses. Thin Silicon cells are embedded into an encapsulating polymer layer (EVA), covered by a much thicker tempered glass [1]. The majority of solar cells available on the market are made of either monocrystalline or polycrystalline Silicon. Solar cells are separated in their plane by a certain amount of EVA. Two main semiconductors, called *busbars*, electrically connect the cells in series. Very thin Aluminum conductors perpendicular to the busbars, called *fingers*,

are also present to collect the electrons originated by the photovoltaic effect from the surface of the semiconductor to the busbars. The microstructure of a typical polycrystalline Silicon cell is shown in Fig. 1, where the two busbars and the geometry of polycrystals are displayed.

Fig. 1: photo of the microstructure of a polycrystalline Silicon solar cell [2].

The quality control of these composites is of primary concern from the industrial point of view. On the one hand, the aim is to develop new manufacturing processes able to reduce the number of cells or modules rejected. On the other hand, even if all the damaged cells are theoretically discarded during manufacturing, it is impossible to avoid the occurrence of microcracking during the subsequent stages. Sources of damage in Silicon cells are transport, installation and use (in particular impacts, snow loads and environmental aging caused by temperature and relative humidity variations) [3-6]. Since microcracking can lead to large electrically disconnected areas, there is an urgent need to understand the origin of this phenomenon and find new technical solutions to improve the durability of PV modules.

To investigate the effect of mechanical loading on cracking in solar cells, mini-modules of 10 cells disposed along two rows (5 cells per row) have been subjected to 4-point bending in [6] (see Fig. 2a). The force-displacement curve obtained from this test is depicted in Fig. 2b and shows brittle failure as soon as cracking propagates. Microcrack patterns, impossible to be detected by a naked-eye inspection of solar cells, have been monitored by using the electroluminescence (EL) technique, see Fig. 3 [6]. These images refer to the portion of the modules where the bending moment is constant. Cracks develop along some preferential lines almost parallel to the direction of line loading. In case of horizontal busbars perpendicular to the line of loading, Fig. 3a, a diffuse crack patter is observed with the apprearance of crack branching. For vertical busbars parallel to the line of loading, Fig. 3b, single cracks propagate and lead to large electrically disconnected black areas. The orientation of busbars and of the thin electric fingers has therefore a role on the crack pattern at failure [6]. Both transgranular and intergranular cracks are present and should be considered in numerical models, although a qualitative visual inspection of Fig. 3 suggests that transgranular cracking is more frequent than the intergranular one.

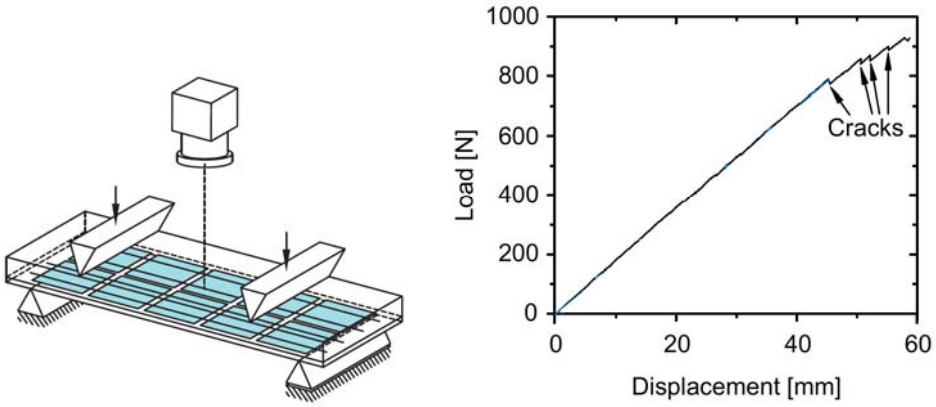

(a) (b)

Fig. 2: Setup of the experimental test on mini-modules (adapted from [6]) and load-displacement curve (b).

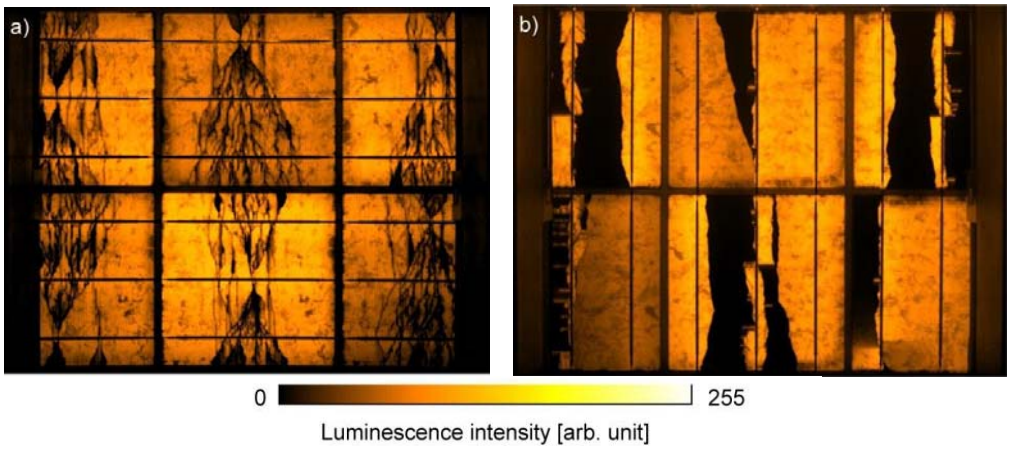

Fig. 3: Microcrack patterns of mini-modules made of polycrystalline Silicon tested according to the test in Fig. 2 (adapted from [6]). (a) Line loading perpendicular to busbars; (b) line loading parallel to busbars.

From the modelling point of view, a multi-physics and multi-scale computational model has been proposed by the present authors in [2]. The original idea is to couple elastic, thermal and electric fields to achieve a predictive stage. To simulate fracture in solar cells of a commercial PV module (composed of up to 60 cells), structural analysis has been performed by using the finite element method and considering the laminate as a multi-layered plate. The computed in-plane displacements at the boundaries of the cells are transferred to the micro-models of the individual cells, where the actual material microstructure is considered. In [2], intergranular cracking has been simulated by inserting cohesive interface elements along the grain boundaries, see an example in Fig. 4 corresponding to the image in Fig. 1. Further progress has been presented in [7], where coupling between the elastic and the thermal fields has been accounted for by developing a staggered solution scheme.

In the present study, transgranular cracking, i.e., cracking through the grains, is also considered in addition to the intergranular one. To this aim, a Matlab pre-processor has been coded to automatically generate finite element (FE) meshes with cohesive interface elements inserted between all the FE edges. Different fracture parameters can be associated to the interface elements depending on their position (along the grain boundaries or inside the grains). Numerical examples are provided to show the applicability of this computational approach to polycrystalline Silicon solar cells. Depending on the cohesive properties associated to the grain boundary and grain interior cracks, the computed crack patterns are compared and general trends are determined.

GENERATION OF FINITE ELEMENT MESHES

Finite element meshes are generated according to the following procedure. First, a digital photo of a solar cell is analyzed and its microstructure identified with a Matlab code developed in house. Grain boundaries and grain geometries are stored in topological entities called edges and vertices. This data structure is then passed in input to the free software GMSH [8] for meshing the grains as if they were joined. This operation can be done with linear triangular or quadrilateral finite elements with a prescribed mesh density. The output of GMSH is then elaborated by another Matlab code developed in house. This programme duplicates all the nodes of the finite elements and inserts interface elements all around them. The properties of the interface elements can be finally attributed depending on their position (inside the grains or along the grain boundaries). The final output is represented by the list of nodal coordinates and the elements connectivity matrix in a format suitable for running a simulation with the finite element analysis programme FEAP [9]. Other formats used by commercial FE softwares like Abaqus or Ansys can also be easily produced.

In the present study, we focus our attention on a model problem consisting of 4 grains (lateral size of about 1 cm). Three different FE mesh densities are considered, see Fig. 4. An initial crack is introduced inside one of the grains to localize the deformation. This microstructure is tested under vertical displacement control to simulate crack propagation in tension. Using this intrinsic cohesive fracture approach, where all the interface elements are inserted in the model from the beginning of the simulation, we expect the following features according to the state-of-the-art literature on this subject [10-14]:

(1) Increase of deformability by refining the mesh size.

(2) The fixed orientation of the interface elements can induce mesh-dependent crack patterns for very coarse meshes.

(3) Fine meshes are in general required to resolve the stress field at the crack tip.

The first drawback can be avoided by incresing the initial stiffness of the interface element. In the present study, since we are mostly interested in the crack path, this effect will not be corrected. The second issue is examined by checking the sensitivity of the crack pattern to the mesh size. Finally, the finest mesh size used in this study is expected to provide a reasonable

approximation to the stress field, according to the criteria proposed in [11,13].

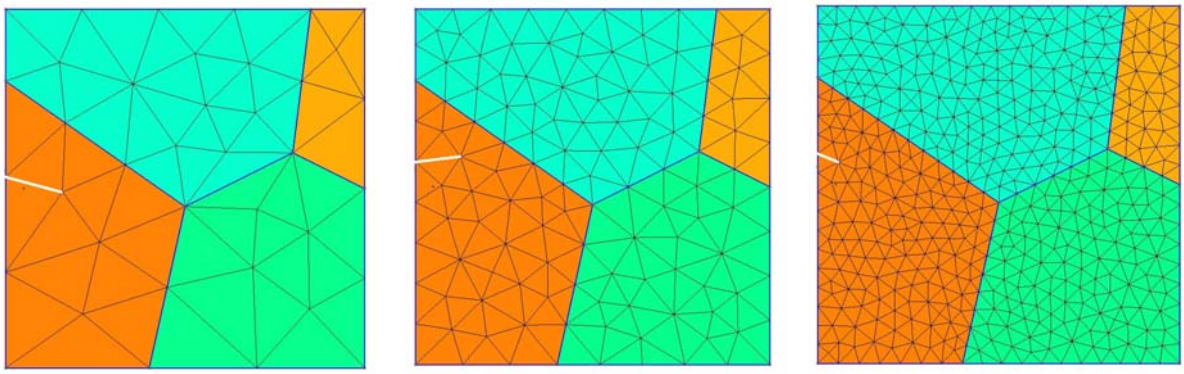

(a) Coarse mesh (b) Intermediate mesh (c) Fine mesh

Fig. 4: FE meshes with different mesh densitites used in the numerical tests. Note the initial crack inserted in the orange grain (see the online version of the article for colours).

FINITE ELEMENT FORMULATION

As a first approximation, it is assumed that the in plane displacements are responsible for cracking in PV modules and that bending of the cell can be neglected. Hence, the deformed configuration can be confused with the undeformed one. As a result of this assumption, the actual tridimensional problem is simplified into a bidimensional one. The principle of virtual work reads:

$$\int_V (\nabla \delta \boldsymbol{u})^{\mathrm{T}} \boldsymbol{\sigma} \, \mathrm{d}V - \int_S \delta \boldsymbol{g}^{\mathrm{T}} \boldsymbol{t} \, \mathrm{d}S = \int_{\partial V} \delta \boldsymbol{u}^{\mathrm{T}} \boldsymbol{f} \, \mathrm{d}S, \tag{1}$$

where the first term on the l.h.s. is the classical virtual work of deformation of the bulk V and the r.h.s. is the virtual work of tractions acting on the boundaries of the cell ∂V, if any. The second term on the l.h.s. is the contribution to the virtual work of the vector of the normal and tangential cohesive tractions $\boldsymbol{t}=(\sigma,\tau)^{\mathrm{T}}$ for the corresponding relative opening and sliding displacements $\boldsymbol{g}=(g_{\mathrm{N}},g_{\mathrm{T}})^{\mathrm{T}}$ at all the element boundaries S.

According to the cohesive zone model (CZM), tractions normal and tangential to an interface are opposing to the relative opening and sliding displacements evaluated at the interface level. Here, the Mixed Mode formulation by Tvergaard [15] is adopted, since it is suitable for modelling grain boundary decohesion in polycrystalline materials. The nonlinear equations relating the cohesive tractions to the normal and tangential relative displacements are:

$$\sigma = \frac{g_{\mathrm{N}}}{l_{\mathrm{Nc}}} P(\lambda), \tag{2a}$$

$$\tau = \gamma \frac{g_{\mathrm{T}}}{l_{\mathrm{Tc}}} P(\lambda), \tag{2b}$$

where:

$$P(\lambda) = 27\sigma_{\max}(1 - 2\lambda + \lambda^2)/4 \tag{3a}$$

$$\lambda = \sqrt{(g_N/l_{Nc})^2 + (g_T/l_{Tc})^2}. \tag{3b}$$

The FE discretization of the micro-model is performed by using linear triangular elements for the grains and compatible linear interface elements for the interfaces [16,17]. The discretized interface contribution in Eq. (1) becomes:

$$\Delta\delta W_{\text{int}} = \delta \boldsymbol{u}^{\mathrm{T}} \boldsymbol{R}^{\mathrm{T}} \int_S \boldsymbol{B}^{\mathrm{T}} \boldsymbol{t}\, \mathrm{d}S, \tag{4}$$

where $\delta\boldsymbol{u}=[u_1,v_1,...,u_4,v_4]^{\mathrm{T}}$ is the displacement vector, $\boldsymbol{R}$ is the rotation matrix of the interface element, and the matrix $\boldsymbol{B}$ contains its shape functions:

$$\boldsymbol{B} = \begin{bmatrix} -N_1 & 0 & -N_2 & 0 & N_2 & 0 & N_1 & 0 \\ 0 & -N_1 & 0 & -N_2 & 0 & N_2 & 0 & N_1 \end{bmatrix} \tag{5}$$

Due to the nonlinearity of the interface constitutive relation given by the CZM, the Newton–Raphson scheme is used, which allows to achieve a quadratic convergence in the computation. The reader is referred to [17] for more details about the computational issues. In this context, linearization of Eq.(22) yields

$$\Delta\delta W_{\text{int}} = \delta \boldsymbol{u}^{\mathrm{T}} \boldsymbol{R}^{\mathrm{T}} \int_S \boldsymbol{B}^{\mathrm{T}} \boldsymbol{C}\boldsymbol{B}\boldsymbol{R}\boldsymbol{u}\, \mathrm{d}S, \tag{6}$$

where $\boldsymbol{C}$ is the tangent constitutive matrix of the interface element containing the partial derivatives of the cohesive tractions w.r.t. the opening and sliding relative displacements [17].

NUMERICAL RESULTS

Two sets of numerical simulations are performed by selecting different fracture properties of the interface elements. The portion of the material microstructure whose geometry is shown in Fig. 4 is subjected to a tensile test in the vertical direction under displacement control. Regarding the computational effort, the finest meshes require approximately 1 hour of computing time.

In the first set, all the interface elements have the same fracture properties, regardless of their position. For the coarse mesh, Fig. 5(a), the initial defect propagates inside the orange and blue grains by crossing their grain boundary. When the crack impinges into the triple junction between the green, yellow and blue grains, it deviates along the grain boundary between the green and the yellow grains (refer to Fig. 4 for the grain color). By refining the mesh, localization is spread out across a larger band, with non zero opening displacements in all the interface elements in the band around the main crack path, which is almost the same as in case (a). The homogenized stress-displacement curves, normalized by dividing the plotted

values by the peak stress and displacement values of the coarse mesh simulation, are shown in Fig. 5. The response is quite brittle, due to the appearance of instabilities in the material microstructures (snap-back instabilities) that cannot be controlled under displacement control. The peak stress is slightly reduced by refining the mesh size.

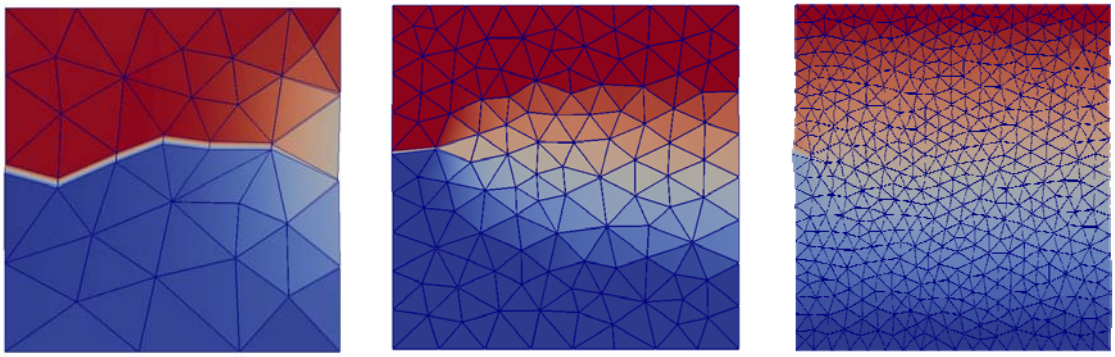

(a) Coarse mesh (b) Intermediate mesh (c) Fine mesh

Fig. 5: contour plot of the vertical displacements at failure, showing displacement discontinuities and a reduction of strain localization by refining the FE mesh.

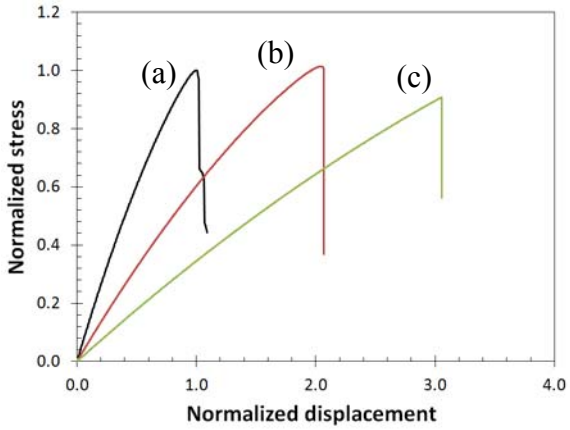

Fig. 6: dimensionless stress-displacement curves corresponding to the FE simulations in Fig. 5. The coarser the FE mesh, the stiffer the mechanical response (less interface elements embedded in the FE mesh).

In the second set, to simulate the phenomenon of intergranular cracking, the fracture properties of the interface elements along the grain boundaries are progressively reduced. Grain boundary decohesion is observed for very weak grain boundaries (fracture toughness less than one fifth of that associated to the grains). In this case, the initial defect does not propagate, whereas debonding of the grain boundary between the orange and the blue grains takes place (see Fig. 7). The final crack pattern shows grain boundary decohesion regardless of the mesh size. The dimensionless stress-displacement curves are shown in Fig. 8 and have

a peak stress about 1/3 of that in Fig. 6 for transgranular cracking.

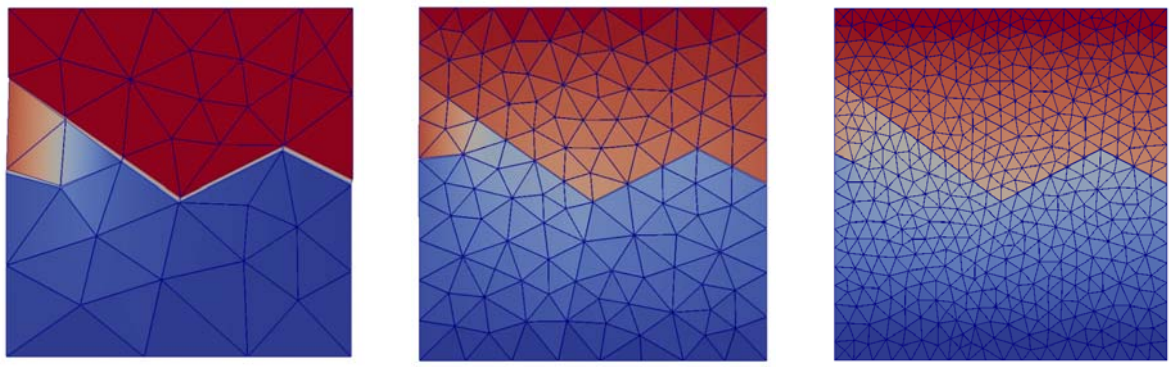

(a) Coarse mesh (b) Intermediate mesh (c) Fine mesh

Fig. 7: contour plot of the vertical displacements at failure, showing displacements discontinuities. The crack pattern is almost independent of mesh refinement.

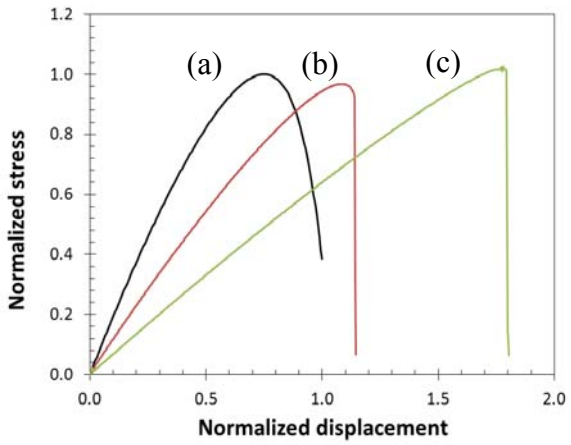

Fig. 8: dimensionless stress-displacement curves corresponding to the FE simulations in Fig. 7. The coarser the FE mesh, the stiffer the mechanical response (less interface elements embedded in the FE mesh).

CONCLUSIONS

A computationl framework for the study of intergranular and transgranular cracking in monocrystalline and polycrystalline Silicon solar cells has been proposed in the present work. To this aim, a specific Matlab pre-processor has been developed in house and has been used to generate FE meshes with embedded interface elements. At present, a full Newton-Raphson technique has been used to solve the nonlinear boundary value problem. However, to capture unstable branches and follow the post-peak response, other special control procedures will be exploited in future work.

Numerical results show a clear prevalence of transgranular cracking over intergranular fracture, as also observed in experimental tests [6]. Pure intergranular cracking is expected only for very weak grain boundaries. This pinpoints the necessity of simulating transgranular cracking in real solar cells, although the computational cost and convergence problems are enhanced.

Indeed, further research is required for the study of convergence issues depending on the CZM stiffness and mesh size. The presence of fingers and busbars will also be accounted for as a global toughening effect. Identification of CZM parameters is also expected to be crucial for reproducing the experimental stress-displacement curves in close detail.

ACKNOWLEDGMENTS

The research leading to these results has received funding from the European Research Council under the European Union's Seventh Framework Programme (FP/2007–2013)/ERC Grant Agreement No. 306622 (ERC Starting Grant "Multi-field and Multi-scale Computational Approach to Design and Durability of PhotoVoltaic Modules" – CA2PVM). The support of the Italian Ministry of Education, University and Research to the Project FIRB 2010 Future in Research "Structural mechanics models for renewable energy applications" (RBFR107AKG) is also gratefully acknowledged.

REFERENCES

[1] M. Paggi, S. Kajari-Schröder and U. Eitner. Thermomechanical deformations in photovoltaic laminates. *Journal of Strain Analysis for Engineering Design* 46, 772–782, 2011.

[2] M. Paggi, M. Corrado and M.A. Rodriguez. A multi-physics and multi-scale numerical approach to microcracking and power-loss in photovoltaic modules. *Composite Structures* 95, 630–638, 2013.

[3] S. Kajari-Schröder, I. Kunze, U. Eitner and M. Köntges. Spatial and orientational distribution of cracks in crystalline photovoltaic modules generated by mechanical load tests. *Solar Energy Materials and Solar Cells* 95, 3054–3059, 2011.

[4] M. Köntges, I. Kunze, S. Kajari-Schröder, X. Breitenmoser and B. Bjrneklett. The risk of power loss in crystalline silicon based photovoltaic modules due to microcracks. *Solar Energy Materials and Solar Cells* 95, 1131–1137, 2011.

[5] S. Kajari-Schröder, I. Kunze, M. Köntges. Criticality of cracks in PV modules. *Energy Procedia* 27, 658–663, 2012.

[6] M. Sander, S. Dietrich, M. Pander, M. Ebert, J. Bagdahn. Systematic investigation of cracks in encapsulated solar cells after mechanical loading. *Solar Energy Materials & Solar Cells* 111, 82–89, 2013.

[7] M. Paggi, A. Sapora. Numerical modelling of microcracking in PV modules induced by thermo-mechanical loads. *Energy Procedia*, 2013, in press.

[8] C. Geuzaine, J.-F. Remacle. Gmsh: a three-dimensional finite element mesh generator with built-in pre- and post-processing facilities. *International Journal for Numerical Methods in Engineering* 79, 1309–1331, 2009.

[9] O.C. Zienkiewicz, R.L. Taylor. *The Finite Element Method*, fifth ed., Butterworth–Heinemann, Oxford and Boston, 2000.

[10] D.V. Kubair, P.H. Geubelle. Comparative analysis of extrinsic and intrinsic cohesive models of dynamic fracture. *International Journal of Solids and Structures* 40, 3853–3868, 2003.

[11] M. Paggi, P. Wriggers. Stiffness and strength of hierarchical polycrystalline materials with imperfect interfaces. *Journal of the Mechanics and Physics of Solids* 60, 557–572, 2012.

[12] H.D. Espinosa, P.D. Zavattieri. A grain level model for the study of failure initiation and evolution in polycrystalline brittle materials. Part I: Theory and numerical implementation. *Mechanics of Materials* 35, 333–364, 2003.

[13] H.D. Espinosa, P.D. Zavattieri. A grain level model fort he study of failure initiation and evolution in polycrystalline brittle materials. Part II: numerical examples. *Mechanics of Materials* 35, 365–394, 2003.

[14] R.H. Kraft, J.F. Molinari. A statistical investigation of the effects of grain boundary properties on transgranular fracture. *Acta Materialia* 56, 4739–4749, 2008.

[15] V. Tvergaard. Effect of fiber debonding in a whisker-reinforced metal. *Materials Science and Engineering* A 107, 23–40, 1990.

[16] M. Paggi, P. Wriggers. A nonlocal cohesive zone model for finite thickness interfaces – Part I: mathematical formulation and validation with molecular dynamics. *Computational Materials Science* 50, 1625–1633, 2011.

[17] M. Paggi, P. Wriggers. A nonlocal cohesive zone model for finite thickness interfaces – Part II: FE implementation and application to polycrystalline materials. *Computational Materials Science* 50, 1634–1643, 2011.